

Study Effects of Seasonal Alterations on Histomorphometrics and Anatomycail Structure of Poll Glands in Male Iraqi Camel (Camelus dromedarius)

 Baqir Rasam Mushir  AHMED J . alyasery

E-mail : baqir.rassam@mu.edu.iq

I. Abstract

This study was conducted to comparatively investigate the morphological, characteristics of the poll gland in adult male dromedary camels during the breeding season (December to March) versus the non-breeding season. Ten sexually mature male camels were used during the breeding season, and ten others during the non-breeding season.

The morphological component of the study involved describing the shape and anatomical location of the poll gland in sexually mature males, along with gross measurements including size, weight, length, width, and thickness. These parameters were analyzed statistically across both seasons.

Morphological findings revealed that the poll gland in adult males consists of two lobes connected by connective tissue enclosed within a distinct capsule. The gland is located subcutaneously in the nuchal region behind the ears and has an ovoid to almond-like irregular shape. Its color ranges from pale pinkish-gray during the breeding season to dark gray or yellowish-brown during the non-breeding season. Histologically, the capsule was composed of two layers: an outer fibrous layer and an inner smooth muscular layer containing smooth muscle cells. Seasonal changes in capsule structure were observed, with significant variations in alveolar lumen diameter and connective tissue thickness between the lobules.

II. Introduction

The genus *Camelus* is one of the basal genera of the Camelidae family, and is closely related to the extinct camel, the Arabian camel (*Camelus dromedarius*). *Camelus* (Latin) means camel, *Dromeus* (Greek) means runner and the suffix *-arius* (Latin) means running camel, hence *dromedarius* (New Latin) means running camel (Al-Mayahi *et al.*, 2024).

The poll glands are situated on the skin on both sides of the first cervical vertebra, just behind the occiput, in an area where the skin is elevated and the mane appears long and sparse. The glandular parenchyma lies within the dermis and consists of multiple almond-colored, pyramidal lobules. During the summer non-estrus season, these glands undergo atrophy. In contrast, during the winter estrus period, the lobules exhibit cyst-like structures and secrete a foul-smelling, viscous fluid through the overlying skin, which becomes (Yang *et al.*, 2020). The accessory genital glands in camels play a crucial role in the reproductive process, as they are the primary contributors to seminal fluid volume. Their secretions account for approximately 60–90% of the total semen volume, providing an optimal environment rich in substrates essential for sperm motility, fertility, and successful transmission to the female reproductive tract. (Saleh *et al.*, 2020). The morphological characteristics of the accessory sex glands vary widely among mammalian species. In the one-humped camel (*Camelus dromedarius*), the accessory glands include the ampulla, prostate, and bulbourethral glands, while the vesicular gland is absent. Anatomically, the vas deferens in camels is divided into two distinct regions: a proximal ductal portion and a distal ampullary portion. The ampullary region, referred to in mammals as the ampulla ductus deferentis, is commonly known as the ampullary gland due to its primary function as a secretory organ. (Mosallam *et al.*, 2020).

III. Material and Methods:

Samples were collected from the poll gland of sexually mature male Arabian camels (*Camelus dromedarius*), ranging in age from 8 to 12 years. The ages of the animals were verified using the dental ageing formula. The study was conducted during two seasons: the breeding season (December to March) and the non-breeding season (May to August).

The total number of animals included in the study was twenty. Samples were collected from different areas of veterinary slaughterhouses in Muthanna and Najaf Governorates, with two visits per week. The samples were transported to the Anatomy, Histology, and Embryology Laboratory at the College of Veterinary Medicine, Muthanna University, within two hours of slaughter. Immediately after slaughter, the poll gland was carefully excised using sterile dissection instruments (scalpel, scissors, forceps), then placed in clean, airtight containers. The samples were kept refrigerated until transported to the laboratory within 1–2 hours.

In the laboratory, the gland underwent a series of morphometric measurements to determine the length, width, weight, volume, and circumference of each gland lobe. These measurements were made using a sensitive electronic balance to measure weight and a Vernier caliper to accurately measure length and width (**Beardsmore, 1998**). Before fixation, morphological observations were recorded regarding the overall anatomy, including the shape, external surface, color, location, and relationships of the poll gland during both the breeding and non-breeding seasons. A mobile phone camera was used to capture images of the gland to illustrate the overall anatomy.

IV. Results and discussions:

4.1. Anatomical Structure of Poll gland of Camel :

The current study showed that the Arabian camel possesses a pair of poll glands known as poll glands. (**Fig .1**) , These glands are found directly behind the ears on either side of the base of head specifically at fronto-parietal suture . (**Fig.3**) These glands were found to be located directly under the skin in the nuchal region surrounded by a layer of subcutaneous tissue (hypodermis) (**Fig.2**) . These finding similar to (**Atoji *et al.* , 1998**) which studied the histochemical and scanning electron microscopic of Poll glands of one humped camel (*Camelus dromedarius*) and (**Ibrahim and Al –Kheraije,2021**) when explained Seasonal morphology and immunoreactivity of cytokeratin and atrial natriuretic peptide in dromedary camel poll glands .

The glands well developed during the mating season and protrude to the surface of the skin secreting a yellowish watery fluid with a pungent unpleasant odor . These secretion turns black upon exposure to air and drips down the camel's neck during estrus and this hyperactivity is attributed to the hormonal influence of testosterone during the mating season . These results explain the most distinctive feature of camel reproduction and this is what researchers as (**Farh *et al.*, 2018**) which confirmed in rutting and non-rutting periods in dromedary camel and (**Al-Saiady *et al.* ,2015**) who demonstrated the presence of androgens in the gland's secretions during this season .

The present study showed that the gland is ovoid to almond-shaped, but its external appearance appears irregular due to lobulated structure giving its external surface an uneven appearance and its color was observed that the gland acquires a pale pinkish-grey color during sexual activity (**Fig . 4**) while it becomes yellowish-brown or dark gray during the non-breeding season (**Fig . 5**) . which is attributed to decreased secretory activity and shrinkage of gland in the absence of hormonal stimulation. These characteristic features are consistent with the findings of (**Purohit *et al.*, 2020**) who explained that the gland was classified as a tubulo-alveolar lobulated sweat gland, somewhat similar to the mammary gland and with (**Padalino *et al.*, 2016**) who described the behavioral indicators to detect estrus phase and poll gland in the dromedary camel .

Table 1 : Anatomical parameters of the poll gland in Arabian camel during the breeding and non-breeding seasons (Mean \pm SE)

Measurement	breeding season			non-breeding season		
	Right	Left	General	Right	Left	General
Length (cm)	8.500 \pm 0.5773	10.750 \pm 0.9474	9.625 \pm 0.7845	6.000 \pm 0.8165	7.000 \pm 0.8165	6.500 \pm 0.8165
Width (cm)	4.600 \pm 0.6218	5.675 \pm 0.6994	5.137 \pm 0.6617	2.675 \pm 0.7804	3.300 \pm 0.6683	2.987 \pm 0.7265
Weight (gm)	56.500 \pm 4.2031	112.000 \pm 4.8304	84.250 \pm 4.5276	21.250 \pm 2.2173	31.750 \pm 2.7537	26.500 \pm 2.4999
Volume (cm ³)	92.750 \pm 4.4253	151.250 \pm 3.7749	122.000 \pm 4.1130	21.500 \pm 2.3804	33.750 \pm 2.2173	27.625 \pm 2.3003
Tickness (μ m)	7.980 \pm 0.3778	2.925 \pm 0.4754	5.453 \pm 0.4294	19.570 \pm 0.4754	20.567 \pm 0.5906	20.069 \pm 0.5361

Table 2 : Anatomical parameters of the poll gland in Arabian camel during the breeding and non-breeding seasons (Mean \pm SE)



Parameter		T-test(Breeding Season	T-test(Non-Breeding Season)	Significant Difference
1	Length (cm)	2.595	1.592	Yes (P < 0.05)
2	Width (cm)	1.5511	0.8365	(P < 0.05)
3	Weight (gm)	3.6628	2.1113	(P < 0.05)
4	Volume (cm3)	6.1026	2.4253	(P < 0.05)
5	Thickness (µm)	2.6247	7.5983	(P < 0.05)

* T-test values for several parameters during breeding and non-breeding seasons and all show significant differences (P < 0.05)

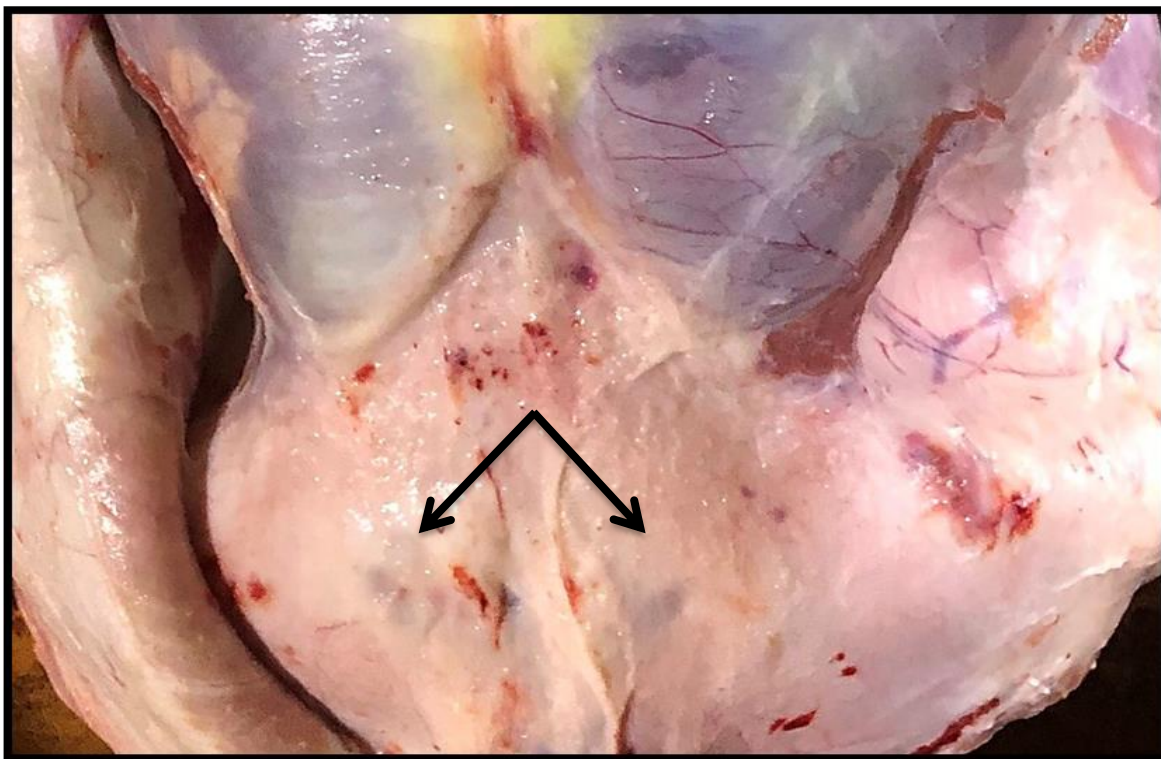


Fig.2. Anatomical Topographic of the Poll Gland in the Camel (*Camelus dromedarius*)

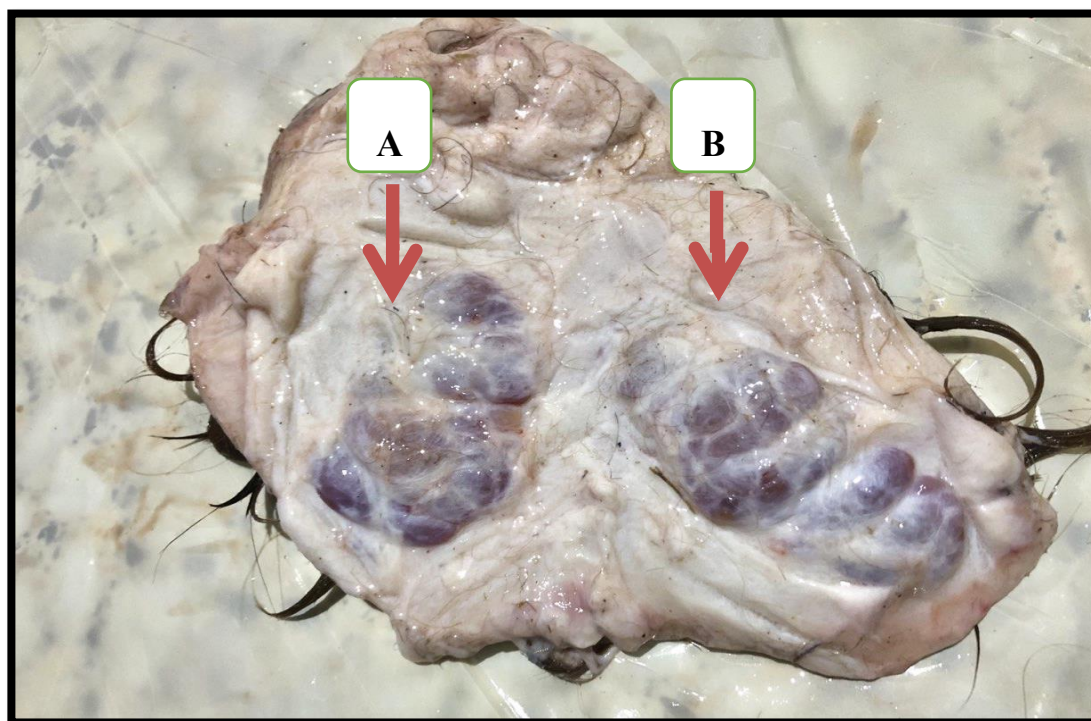


Fig.3. Anatomical Structure of the Poll Gland in the Came l (A) :left ,(B) : Right attached to the skin, with prominent purplish glandular lobules.

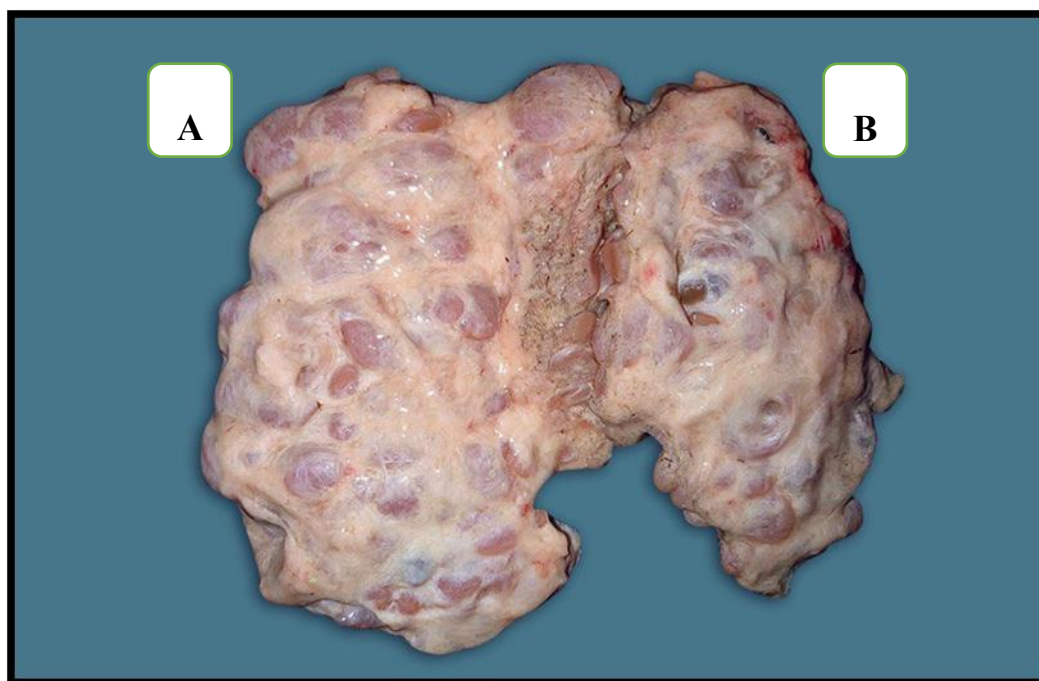


Fig.4. A: Left lobe and B : right lobe , Anatomical Structure of the Poll Gland in the Camel (*Camelus dromedarius*) During the Breeding Season



Fig.5 A: Left lobe and B : right lobe , Anatomical Structure of the Poll Gland in the Camel (*Camelus dromedarius*) During the non_ Breeding Season.

V. References

- AlMayahi, A., Al-Shibli, N., Gibreel, T., Blackburn, D., Al-Ismaily, S., & McHugh, C. (2024). Perceptions and attitudes of farmers and landowners on soil salinity management and use of elemental sulphur in Oman. *Soil Use and Management*, 40(1), e12961.
- Atoji, Y., Yamamoto, Y., & Suzuki, Y. (1998). Morphology of the tongue of a male formosan serow (*Capricornis crispus swinhoei*). *Anatomia, histologia, embryologia*, 27(1), 17-19.
- Bouras, N., Beardsmore, A., Dorman, T., Cooper, S. A., & Webb, T. (1998). Affective psychosis and Prader–Willi syndrome. *Journal of Intellectual Disability Research*, 42(6), 463-471.
- El-Batal, A. I., El-Sayyad, G. S., Mosallam, F. M., & Fathy, R. M. (2020). Penicillium chrysogenum-mediated mycogenic synthesis of copper oxide nanoparticles using gamma rays for in vitro antimicrobial activity against some plant pathogens. *Journal of Cluster Science*, 31, 79-90.

Farh, M. E. A., Kim, Y. J., Kim, Y. J., & Yang, D. C. (2018). Cylandrocarpon destructans/Ilyonectria radicola-species complex: Causative agent of ginseng root-rot disease and rusty symptoms. *Journal of ginseng research*, 42(1), 9-15.

Mousa, W. S., Zaghawa, A. A., Elsify, A. M., Nayel, M. A., Ibrahim, Z. H., Al-Kheraije, K. A., ... & Salama, A. A. (2021). Clinical, histopathological, and molecular characterization of Mycoplasma species in sheep and goats in Egypt. *Veterinary world*, 14(9), 2561.

Padalino, L., Conte, A., & Del Nobile, M. A. (2016). Overview on the general approaches to improve gluten-free pasta and bread. *Foods*, 5(4), 87.

Purohit, B., Vernekar, P. R., Shetti, N. P., & Chandra, P. (2020). Biosensor nanoengineering: Design, operation, and implementation for biomolecular analysis. *Sensors International*, 1, 100040.

Saleh, A., & Mujahiddin, M. (2020). Challenges and opportunities for community empowerment practices in Indonesia during the Covid-19 pandemic through strengthening the role of higher education. *Budapest International Research and Critics Institute-Journal (BIRCI-Journal)*, 3(2), 1105-1113.

Zhao, S., Lin, Q., Ran, J., Musa, S. S., Yang, G., Wang, W., ... & Wang, M. H. (2020). Preliminary estimation of the basic reproduction number of novel coronavirus (2019-nCoV) in China, from 2019 to 2020: A data-driven analysis in the early phase of the outbreak. *International journal of infectious diseases*, 92, 214-217.